

Adsorption of Emerging Munitions Contaminants on Cellulose Surface: A Combined Theoretical and Experimental Investigation

Manoj K. Shukla¹ · Aimee Poda¹

Received: 30 September 2015 / Accepted: 30 March 2016 / Published online: 15 April 2016
© Springer Science+Business Media New York (outside the USA) 2016

Abstract This manuscript reports results of an integrated theoretical and experimental investigation of adsorption of two emerging contaminants (DNAN and FOX-7) and legacy compound TNT on cellulose surface. Cellulose was modeled as trimeric form of the linear chain of 1 → 4 linked of β-D-glucopyranose in ⁴C₁ chair conformation. Geometries of modeled cellulose, munitions compounds and their complexes were optimized at the M06-2X functional level of Density Functional Theory using the 6-31G(d,p) basis set in gas phase and in water solution. The effect of water solution was modeled using the CPCM approach. Nature of potential energy surfaces was ascertained through harmonic vibrational frequency analysis. Interaction energies were corrected for basis set superposition error and the 6-311G(d,p) basis set was used. Molecular electrostatic potential mapping was performed to understand the reactivity of the investigated systems. It was predicted that adsorbates will be weakly adsorbed on the cellulose surface in water solution than in the gas phase.

Keywords 2,4-dinitroanisole (DNAN) · 1,1-diamino-2,2-dinitroethene (FOX-7) · 2,4,6-trinitrotoluene (TNT) · Cellulose · Adsorption · DFT level

Polysaccharides are ubiquitous in nature and they exhibit broad range of variation in their molecular structures and properties. Cellulose is a natural polysaccharide and is a major component of plant cell walls. Cellulose is characterized by the linear chain of 1 → 4 linked polymer of

β-D-glucopyranose in the ⁴C₁ chair conformation. The hydroxyl groups on sugar rings form hydrogen bonds within the same chain and that with neighboring parallel chains. Moreover, due to biodegradable and renewable abilities cellulose is regarded as the greenest available renewable polymeric material on earth (Moon et al. 2011). Armed forces worldwide are developing and adopting insensitive munitions (IM) to avoid accidental and spontaneous detonation of traditional munitions due to shock and high temperature sensitivity at various stages of handling (Felt et al. 2013; Taylor et al. 2015). Obviously, production, storage, training and application of these compounds may lead to their release in the environment and thus may lead to contamination of soils and aquifers and can leach to ground water. Thus, insensitive munition compounds are regarded as emerging contaminants and therefore their fate and transport need to be rigorously investigated.

Therefore, it is logical to thoroughly investigate the sorption of these emerging contaminants on easily available cellulosic biomass. Such investigation may not only shed light on their fate and transport; they can also lead to development of remediation and sensing technologies. For example, cellulose fibers have long been served as raw material in the textile and paper industries or in composite material as filler (Bledzki and Gassan 1999) and have been a major part of composting in bioremediation processes (Thorn et al. 2002). In this manuscript, we have investigated the sorption of two emerging contaminants such as 2,4-dinitroanisole (DNAN), 1,1-diamino-2,2-dinitroethene (FOX-7) and legacy compound 2,4,6-trinitrotoluene (TNT) on cellulose surfaces using a combined Density Functional Theory (DFT) level theoretical and experimental approaches. In the theoretical investigation, cellulose was modeled as the trimeric form of the linear chain of 1 → 4

✉ Manoj K. Shukla
Manoj.K.Shukla@usace.army.mil

¹ Environmental Laboratory, Engineer Research and Development Center, Vicksburg, MS 39180, USA

linked of β -D-glucopyranos in the 4C_1 chair conformation. It was revealed that investigated contaminants will be weakly adsorbed on cellulose surface in the water solution.

Materials and Methods

Geometries of modeled cellulose in the form of trimer of 1 \rightarrow 4 linked linear chain of β -D-glucopyranos, hereafter called modeled cellulose, and adsorbates (DNAN, FOX-7 and TNT) and modeled cellulose-adsorbate complexes were optimized using M06-2X meta-hybrid Density Functional Theory (DFT) functional and the 6-31G(d,p) basis set both in the gas phase and in the bulk water solution. Nature of potential energy surfaces (PESs) of optimized structures was ascertained through calculation of harmonic vibrational frequency analysis; all geometries were found to be minima at the respective PES. Effect of bulk water solvation was modeled using the CPCM approach (Cossi et al. 2003). Interaction energies between the adsorbate and adsorbent in the gas phase were computed at the same theoretical level and using the 6-311G(d,p) basis set and were corrected for basis set superposition error using counterpoise correction scheme (Boys and Bernardi 1970). The interaction energies of complexes in the bulk water solution (hereafter called BSSE corrected interaction energy in bulk water) were obtained using the formula:

$$\Delta E_{\text{Int}}(\text{CPCM}) = E_{\text{AB}}(\text{CPCM}) - E_{\text{A}}(\text{CPCM}) - E_{\text{B}}(\text{CPCM}) + \text{BSSE}_{\text{gas}}$$

where $E_{\text{AB}}(\text{CPCM})$ represents the total energy of the complex in the bulk water, $E_{\text{A}}(\text{CPCM})$ and $E_{\text{B}}(\text{CPCM})$ represent the total energy of the monomer A and B respectively in the bulk water within the complex geometry optimized in water and BSSE_{gas} represents the basis set superposition energy correction obtained from the gas phase calculation using the counterpoise correction scheme. All calculations were performed using Gaussian 09 program (Frisch et al. 2009).

An E4 (QCM-D, Q-Sense AB) was used to measure adsorption of DNAN, FOX-7 and TNT onto thin cellulose films. Cellulose sensors (QX 334) and Silicon (QX 301) were purchased directly from Biolin scientific and used as received. The cellulose coating on the QX 334 sensors was based on work done by Pääkkö et al. (2007) and the films consist of isolated cellulose fibers from softwood cellulose pulp (Domsjo ECO Bright; Domsjo Fabriker AB). The material specifications indicate that the cellulose film is made from nanofibular cellulose with both crystalline cellulose I and amorphous regions with a Poly (ethylene imine) adhesive layer that ranges in thickness

between 5 and 6 nm between the cellulose fibers and silicon surface. The reported nanofibular cellulose thickness is 6 nm with some fibril aggregates sizing between 10 and 20 μm . Surfaces were imaged in tapping mode with a Dimension Icon Atomic force Microscope (Bruker) and height images were collected under ambient conditions with a silicon tip (TAP150A Part: MPP-1(2120-10)). The reported root mean square (RMS) roughness were determined from 5 μm \times 5 μm scan areas. The cellulose film was fibrous in nature as discussed in the “Results and Discussion” section. The RMS roughness for these films was 3.1 ± 0.5 nm.

Water Uptake Total water content of the saturated cellulose film was determined with a QCM-D and a $\text{H}_2\text{O}/\text{D}_2\text{O}$ solvent exchange procedure (Fält et al. 2003). The water content of the thin films was determined using a previously published technique in which the scaled frequency shift caused by switching the solvent from deionized water (H_2O) to deuterium oxide (D_2O) is used to measure the water within the film (Craig and Plunkett 2003). For this comparison a *bare* uncoated silicon crystal was subjected to the identical procedure as the cellulose *film* sensor. The utilization of a bare crystal allowed for compensation of the density changes between D_2O and H_2O . For this method, $(\Delta f/n)_{\text{water}}$ can be calculated from the difference between $(\Delta f/n)_{\text{film}}$ and $(\Delta f/n)_{\text{bare}}$:

$$\left(\frac{\Delta f}{n}\right)_{\text{water}} = \frac{\left(\frac{\Delta f}{n}\right)_{\text{film}} - \left(\frac{\Delta f}{n}\right)_{\text{bare}}}{\left(\frac{\rho_{\text{D}_2\text{O}}}{\rho_{\text{H}_2\text{O}}}\right) - 1} \quad (1)$$

where $\rho_{\text{D}_2\text{O}}$ and $\rho_{\text{H}_2\text{O}}$ are the densities of D_2O and H_2O , respectively at 25°C. The constant C is defined as the Sauerbrey constant (0.177 mg s m^{-2}). Thus, $(\Delta f/n)_{\text{water}}$ from Eq. 1 can be used to calculate the $[\Gamma_{\text{water}}]$ “surface concentration” of water in the film through a Sauerbrey relationship (1959):

$$\Gamma_{\text{water}} = C \left(\frac{\Delta f}{n}\right)_{\text{water}} \quad (2)$$

Adsorption Data Deionized water was introduced into the flow cell at a rate of 0.150 mL min^{-1} at 25°C until a stable baseline was obtained. During this period of water introduction baseline stabilization corresponded to maximum water uptake associated with the cellulose films. After stabilization the deionized water was switched to D_2O and allowed to equilibrate. After equilibration the D_2O was exchanged for deionized water until baseline stabilization was re-acquired. Figure 4 shows representative plots of $(\Delta f/n)$ versus time, t , for a silicon sensor and a silicon sensor coated with a 6.0 nm film of cellulose switched from H_2O to D_2O and back to H_2O . Values of Γ_{water} were calculated from QCM results (see “Results

and Discussion” section) using Eqs. 1 and 2. After re-stabilization in deionized water, adsorbate solutions (50 ppm in deionized water) was introduced into the flow cell at the same rate and temperature as the deionized water and the change in frequency was recorded (Marx 2003).

Results and Discussion

Optimized geometries of modeled cellulose and adsorbates (DNAN, FOX-7, and TNT) at the M06-2X/6-31G(d,p) level along with their numbering schemes and some selected geometrical parameters are shown in the Fig. 1. In the modeled cellulose, the trimeric form of β -D-glucopyranos in the 4C_1 chair conformation in 1 \rightarrow 4 linear chain linkage was considered. Moreover, the terminal $-OH$ groups were replaced with $-OCH_3$ group to avoid their interaction with adsorbates. Selection of such model was to avoid computational cost and moreover the size of the model cellulose system was sufficient considering the size of adsorbates under investigation. Selected computed dihedral angles of modeled cellulose are shown in the Table 1. The corresponding geometrical parameters of cellulose I_β form obtained from the X-ray and neutron diffraction data (Nishiyama et al. 2002) are also shown in the Table 1. Computed geometrical parameters can be regarded in good agreement with the experimental data. The obtained disagreement (Table 1) is due to the fact that

Table 1 Computed and experimental (cellulose I_β) geometrical parameters of cellulose

Parameters	Computed		Experimental ^a
	Gas phase	Bulk water solution	
C1O5C5C4	62.3	62.3	54.8
O5C5C4C3	-59.4	-59.5	-55.3
C5C4C3C2	55.3	56.2	57.2
O1C1O5C5	-178.7	-178.4	-169.1

^a Nishiyama et al. (2002). Parameters were obtained from the cif file

experimental data belong to the crystalline form of cellulose I_β where conformational movements are significantly restricted due to the presence of inter-chain hydrogen bonds. Theoretical calculation performed in this work predicted that modeled cellulose will have similar conformation both in the gas phase and in the bulk water solution.

Computed gas phase and in the bulk water solution bond lengths of adsorbates are shown in the Table 2. The experimentally determined bond lengths using X-ray crystallography are also shown in the same table. We would like to point out that for DNAN and TNT two different geometries with equal probability was predicted experimentally (Nyburg et al. 1987; Carper et al. 1982) and bond lengths for both (presented as A and B in the Table 2) are shown in the table. For FOX-7, the experimental bond lengths shown in Table 2 were obtained from the

Fig. 1 Geometry and atomic numbering schemes of investigated system

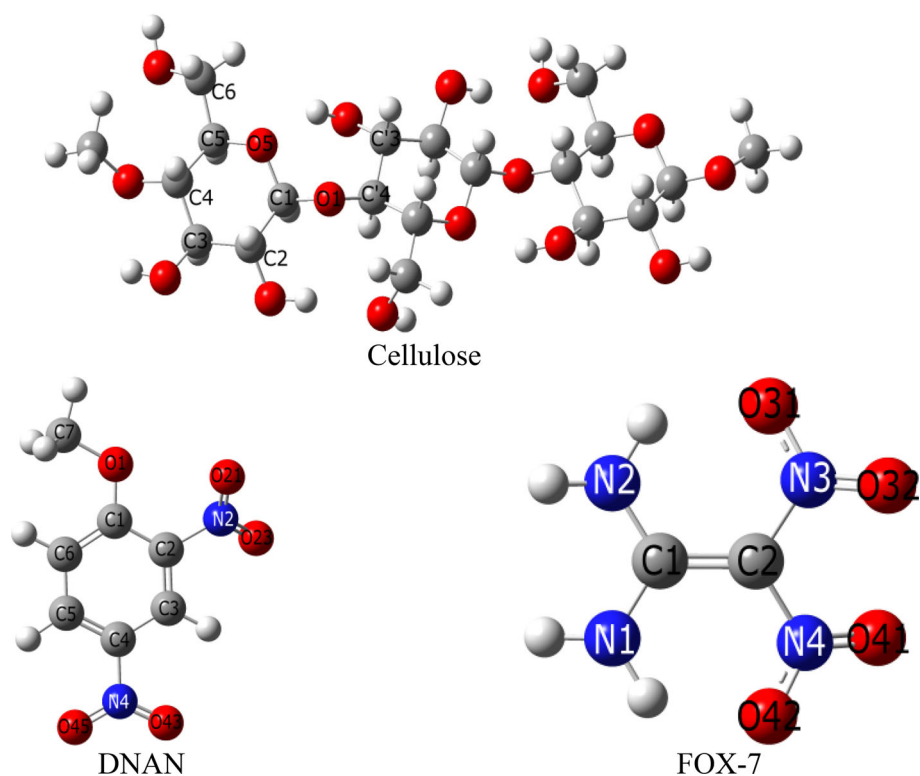


Table 2 Computed and experimental geometrical parameters of adsorbates, their dipole moments (μ , in Debye) and BSSE corrected interaction energies (ΔE_{int} , kcal/mol)

Parameters	Theoretical		Experimental		Parameters	Theoretical		Experimental	
	Gas	Water	A	B		Gas	Water	A	B
DNAN ^a					TNT ^b				
C1-C2	1.411	1.414	1.402	1.393	C1-C2	1.404	1.404	1.390	1.395
C2-C3	1.382	1.383	1.361	1.374	C2-C3	1.386	1.386	1.364	1.383
C3-C4	1.385	1.384	1.388	1.360	C3-C4	1.382	1.382	1.415	1.344
C4-C5	1.387	1.391	1.369	1.376	C4-C5	1.382	1.382	1.375	1.373
C5-C6	1.386	1.384	1.372	1.380	C5-C6	1.386	1.386	1.373	1.387
C6-C1	1.403	1.405	1.377	1.387	C6-C1	1.404	1.404	1.408	1.379
C1-O1	1.333	1.328	1.333	1.338	C1-C7	1.507	1.505	1.505	1.507
C7-O1	1.419	1.428	1.436	1.447	C2-N2	1.477	1.474	1.496	1.459
C2-N2	1.470	1.463	1.475	1.454	C4-N4	1.473	1.468	1.443	1.482
N2-O21	1.213	1.216	1.188	1.208	C6-N6	1.477	1.474	1.449	1.494
N2-O23	1.218	1.221	1.190	1.271	μ	1.43	1.69		
C4-N4	1.465	1.459	1.468	1.478	ΔE_{int}	-26.3	-16.7		
N4-O43	1.216	1.219	1.211	1.212	FOX-7 ^c				
N4-O45	1.217	1.219	1.212	1.210	C1-C2	1.416	1.441	1.456	
μ	6.56	8.33			C1-N1	1.341	1.329	1.325	
ΔE_{int}	-20.0	-11.7			C1-N2	1.341	1.329	1.319	
					C2-N3	1.429	1.417	1.398	
					C2-N4	1.429	1.417	1.426	
					N3-O31	1.240	1.239	1.249	
					N3-O32	1.211	1.220	1.252	
					N4-O41	1.211	1.220	1.242	
					N4-O42	1.240	1.239	1.242	
					μ	8.36	11.61		
					ΔE_{int}	-29.2	-18.3		

^a See reference Nyburg et al. (1987), ^b Carper et al. (1982), ^c Bemm and Ostmark (1998). Experimental parameters for FOX-7 were determined from the corresponding cif file

corresponding cif files (Bemm and Ostmark 1998). It is evident from the data shown in the Table 2 that noticeable change between computed bond length in the gas phase and in the bulk water solution is not revealed. Further, the computed bond lengths are generally in good agreement with the corresponding experimental data and small disagreement can be accounted to the crystal environment in the X-ray crystallographic measurement. Computed dipole moment of considered adsorbates in the gas phase and in the bulk water solution are shown in the Table 2. It is clear from this table that comparison to the gas phase, dipole moments in the bulk water solution are generally larger. Moreover, our calculation predicted that FOX-7 has the largest and TNT has the lowest dipole moment.

Molecular electrostatic potential (MEP) is an important property which is related to the reactivity of molecular system (Politzer et al. 1985). Computed MEP map plotted on electron density of modeled cellulose and adsorbates are shown in the Fig. 2. It is clear from this figure that negative

potential regions are located at lone pair site of oxygen centers. And therefore, it is not unexpected that most negative potentials are predicted to be oxygen atoms of nitro groups and that of the hydroxyl groups. Moreover, among adsorbates, FOX-7 has been predicted to have the most negative potential while TNT has the least negative potential. Based upon the computed negative potential FOX-7 can be speculated to be adsorbed on cellulose surface stronger than other adsorbates. However, adsorption is complicated process and number of bonding centers and type of interaction play prominent role in such complexation.

Geometries of optimized complexes obtained by adsorption of adsorbates on cellulose surface are shown in Fig. 3. Initial geometries of these complexes were obtained by putting adsorbates in proper orientation which can maximized the number of bonds between the surface and the adsorbates and then completely relaxing complex geometries at the M06-2X/6-31G(d,p) level. Moreover, molecules

Fig. 2 Molecular electrostatic potential (MEP) maps of modeled cellulose and adsorbates mapped on to electron density. The isosurface value is 0.006 and range for MEP for each system is next to their name in the unit of Hartree. *Blue color* shows the region of negative potential and *red color* shows the region of positive potential (Color figure online)

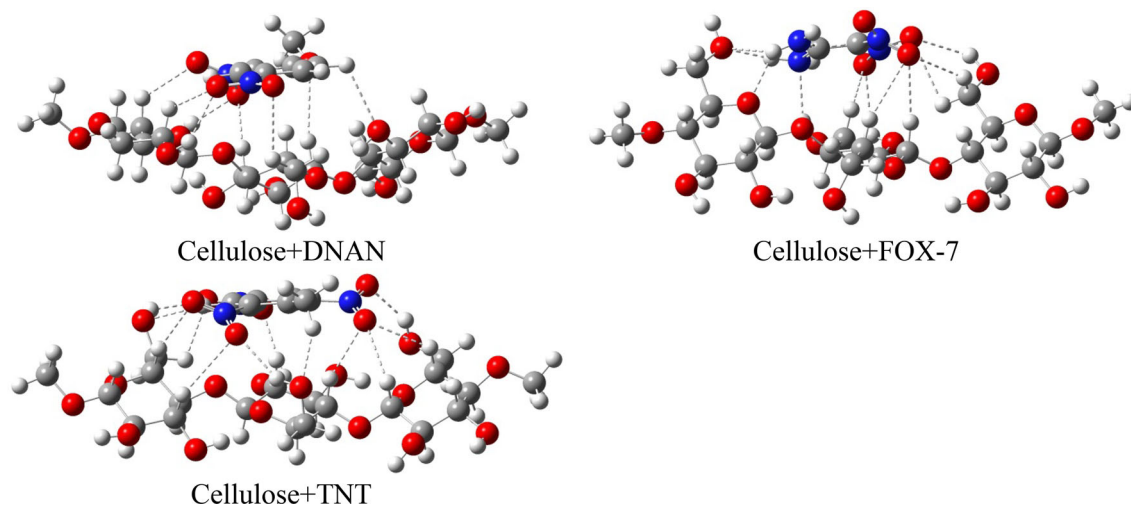
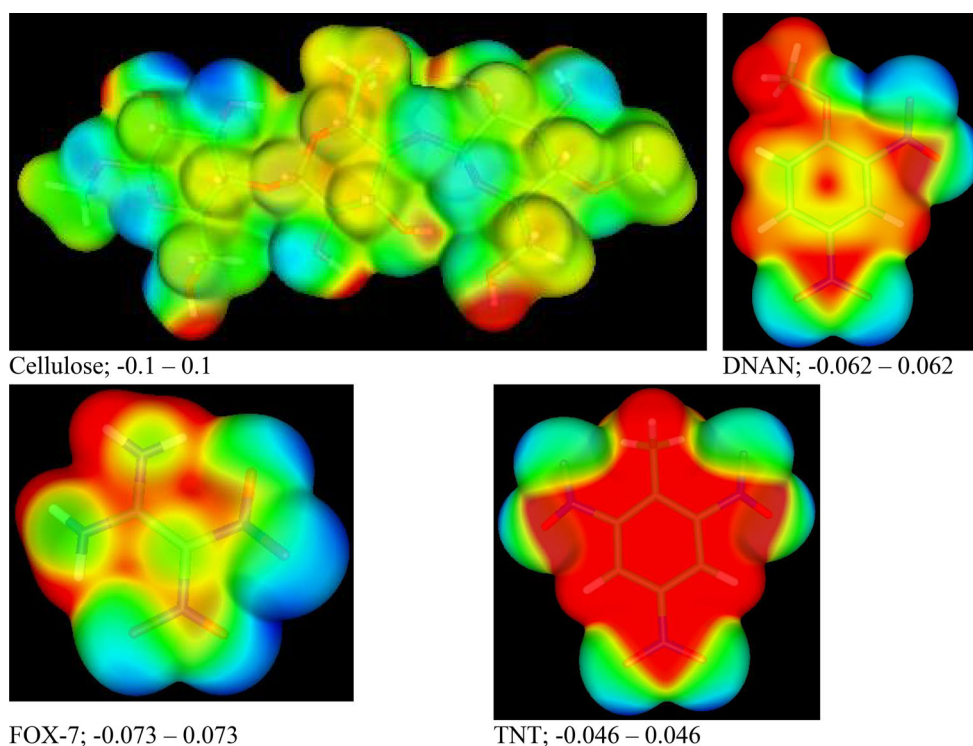


Fig. 3 Optimized geometries of complexes in the bulk water solution

were adsorbed on both sides of the modeled cellulose and complex with higher interaction energy is considered. We would like to state that there are several arrangements for the interaction of adsorbates on cellulose surface, but only one orientation of adsorbates with respect to surface was considered for each of the munitions compounds. It is evident that these complexes are stabilized by the presence of several hydrogen bonds between hydrogen bond accepting and donating sites of adsorbates with the complementary sites of the surface. Moreover, these hydrogen bond distances were

predicted to be in the range of 2.046–2.874 Å for DNAN, 1.924–2.920 Å for FOX-7, and 2.004–2.945 for TNT in the gas phase and 2.028–2.908 Å for DNAN, 1.902–2.886 Å for FOX-7, and 2.002–2.928 for TNT in the bulk water solution. Computed BSSE corrected interaction energies of investigated complexes are shown in the Table 2. It is clear from the data shown in the Table 2 that FOX-7 would form the strongest complex while the DNAN will form the weakest complex on the cellulose surface. Moreover, such binding was found to be significantly decreased in the bulk water

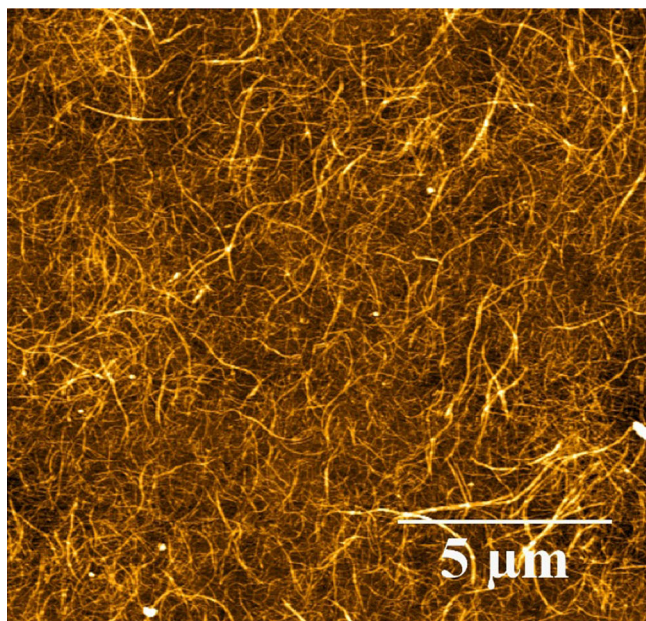
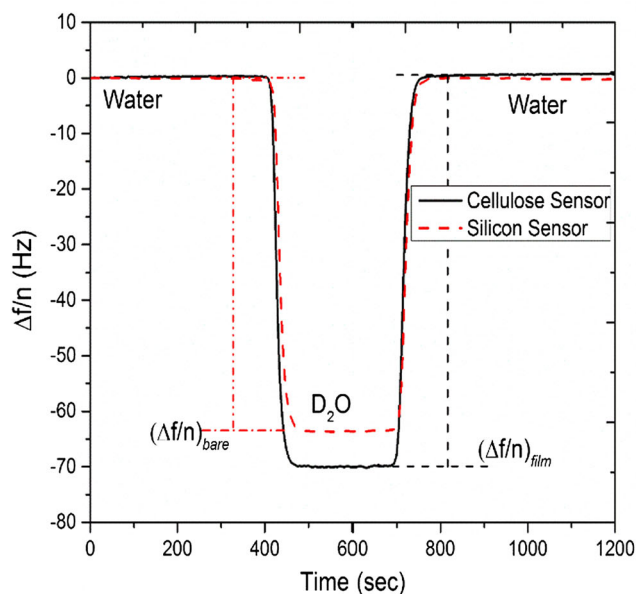


Fig. 4 (Right) Change in resonance frequency due to the adsorption of water on cellulose surface and bare silicon surface using solvent exchange QCM-D experiment. Representative 3rd overtone for bare



silica (black/solid) and silicon sensor (red/dashed). (Left) AFM image of cellulose sensor surface $15 \mu\text{m} \times 15 \mu\text{m}$ (Color figure online)

solution compared to the gas phase. Further, it is evident from the Fig. 3 and data shown in the Table 2 that adsorption of considered energetic compounds on the cellulose surface is weak and such adsorption is dominated by the weak hydrogen bonding interactions. This conclusion is also supported from the QCM-D experiment which suggested low adsorption of investigated energetic molecules. The QCM-D water exchange experiments as represented in Fig. 4 showed that there was a significant amount of water adsorption in the cellulose films with a total surface concentration of water for the cellulose films found to be $4.12 \pm 0.7 \text{ mg/m}^2$. The frequency change observed for the sorbent solutions in the QCM-D experiment which is related to the adsorbed mass was measured. The measured amount of surface adsorption from the sorbent solutions was significantly lower with the mass uptake for TNT measuring 0.108 mg/m^2 , DNAN measuring 0.0242 mg/m^2 and FOX 7 measuring 0.121 mg/m^2 and the results are depicted in Fig. 5. Different frequency responses were observed for each explosive solution. The highest adsorption response was obtained from FOX7 with a frequency change reaching equilibrium quickly. TNT showed a similar amount of adsorption as compared to FOX-7 but never reached equilibrium during the time of contact. Such phenomena may be related to the relatively lower solubility of TNT in water. Minor sorption of DNAN was observed on the cellulose surface.

We have investigated the adsorption of emerging contaminants (DNAN and FOX-7) and legacy compound TNT

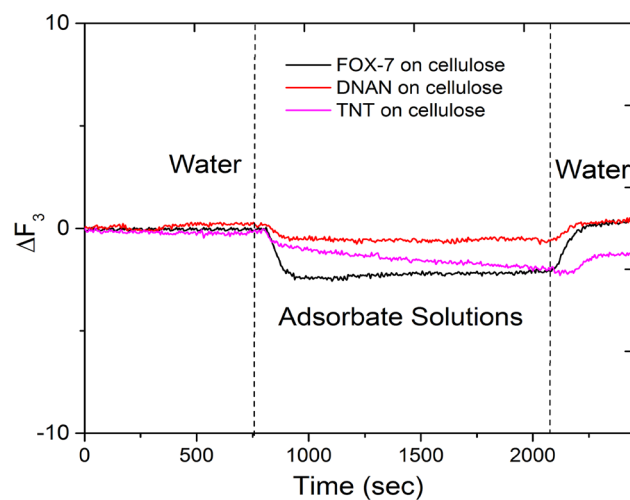


Fig. 5 Change in resonance frequency due to the adsorption of energetics compounds on nanocellulose surface using QCM-D experiment

on cellulose surface using DFT level of theoretical and QCM-D experimental methods. It was found that such adsorption on cellulose surface would be significantly decreased in the bulk water solution compared to that in the gas phase. Moreover, all adsorptions were characterized by the presence of weak hydrogen bonds between adsorbates and adsorbent surface and thus adsorption was predicted to be weak. Among the investigated compounds, the FOX-7 was found to have slightly stronger binding on the cellulose

surface. The cellulose films showed much higher water uptake as compared to the adsorbate solutions.

Acknowledgments The use of trade, product, or firm names in this report is for descriptive purposes only and does not imply endorsement by the U.S. Government. The tests described and the resulting data presented herein, unless otherwise noted, were obtained from research conducted under the Environmental Quality Technology Program of the United States Army Corps of Engineers and the Environmental Security Technology Certification Program of the Department of Defense by the USAERDC. Permission was granted by the Chief of Engineers to publish this information. The findings of this report are not to be construed as an official Department of the Army position unless so designated by other authorized documents. The authors thank Dr. Guilherme Lotufo, and Dr. Chris Griggs of USACE for their editorial comments.

References

- Bemm U, Ostmark H (1998) 1,1-Diamino-2,2-dinitroethylene: a novel energetic material with infinite layers in two dimensions. *Acta Cryst C* 54:1997–1999
- Bledzki AK, Gassan J (1999) Composites reinforced with cellulose based fibers. *Prog Polym Sci* 24:221–274
- Boys SF, Bernardi F (1970) Calculation of small molecular interactions by differences of separate total energies—some procedures with reduced errors. *Mol Phys* 19:553–566
- Carper WR, Davis LP, Extine MW (1982) Molecular structure of 2,4,6-trinitrotoluene. *J Phys Chem* 86:459–462
- Cossi M, Rega N, Scalmani G, Barone V (2003) Energies, structures, and electronic properties of molecules in solution with the C-PCM solvation model. *J Comp Chem* 24:669–681
- Craig VSJ, Plunkett MJ (2003) Determination of coupled solvent mass in quartz crystal microbalance measurements using deuterated solvents. *J Colloid Interface Sci* 262:126–129
- Fält S, Wågberg L, Vesterlind E-L (2003) Swelling of model films of cellulose having different charge densities and comparison to the swelling behavior of corresponding fibers. *Langmuir* 19:7895–7903
- Felt DR, Johnson JL, Larson S, Hubbard B, Henry K, Nestler C, Ballard JH (2013) Evaluation of treatment technologies for wastewater from insensitive munitions production phase I: technology down-selection. U.S. Army Engineer Research and Development Center, ERDC/EL TR-13-20, Vicksburg
- Frisch MJ, Trucks GW, Schlegel HB, Scuseria GE, Robb MA, Cheeseman JR, Scalmani G, Barone V, Mennucci B, Petersson GA, Nakatsuji H, Caricato M, Li X, Hratchian HP, Izmaylov AF, Bloino J, Zheng G, Sonnenberg JL, Hada M, Ehara M, Toyota K, Fukuda R, Hasegawa J, Ishida M, Nakajima T, Honda Y, Kitao O, Nakai H, Vreven T, Montgomery JA Jr, Peralta JE, Ogliaro F, Bearpark M, Heyd JJ, Brothers E, Kudin KN, Staroverov VN, Kobayashi R, Normand J, Raghavachari K, Rendell A, Burant JC, Iyengar SS, Tomasi J, Cossi M, Rega N, Millam JM, Klene M, Knox JE, Cross JB, Bakken V, Adamo C, Jaramillo J, Gomperts R, Stratmann RE, Yazyev O, Austin AJ, Cammi R, Pomelli C, Ochterski JW, Martin RL, Morokuma K, Zakrzewski VG, Voth GA, Salvador P, Dannenberg JJ, Dapprich S, Daniels AD, Farkas Ö, Foresman JB, Ortiz JV, Cioslowski J, Fox DJ (2009) Gaussian 09, revision A.1. Gaussian Inc., Wallingford
- Marx KA (2003) Quartz crystal microbalance: a useful tool for studying thin polymer films and complex biomolecular systems at the solution-surface interface. *Biomacromol* 4:1099–1120
- Moon RJ, Martini A, Nairn J, Simonsen J, Youngblood J (2011) Cellulose nanomaterials review: structure, properties and nanocomposites. *Chem Soc Rev* 40:3941–3994
- Nishiyama Y, Langan P, Chanzy H (2002) Crystal structure and hydrogen-bonding system in cellulose I_β from synchrotron X-ray and neutron fiber diffraction. *J Am Chem Soc* 124:9074–9082
- Nyburg SC, Faerman CH, Prasad L, Palleros D, Nudelman N (1987) Structures of 2,4-dinitroanisole and 2,6-dinitroanisole. *Acta Cryst C* 43:686–689
- Pääkkö M, Ankerfors M, Kosonen H, Nykanen A, Ahola S, Osterberg M, Ruokolainen J, Laine J, Larsson PT, Ikkala O, Lindstrom T (2007) Enzymatic hydrolysis combined with mechanical shearing and high-pressure homogenization for nanoscale cellulose fibrils and strong gels. *Biomacromolecules* 6:1934–1941
- Politzer P, Laurence PR, Jayasuriya K (1985) Molecular electrostatic potentials: an effective tool for the elucidation of biochemical phenomena. *Environ Health Perspect* 61:191–202
- Sauerbrey G (1959) Verwendung von Schwingquarzen zur Wagung dünner Schichten und zur Mikrowagung. *Zeitschrift für Physik* 155:206–222
- Taylor S, Park E, Bullion K, Dontsova K (2015) Dissolution of three insensitive munitions formulations. *Chemosphere* 119:342–348
- Thorn KA, Pennington JC, Hyes CA (2002) ¹⁵N NMR investigation of the reduction and binding of TNT in an aerobic bench scale reactor simulating windrow composting. *Environ Sci Technol* 36:3797–3805